Sustainable Energy & Fuels

ROYAL SOCIETY OF CHEMISTRY

REVIEW

View Article Online
View Journal | View Issue

Cite this: *Sustainable Energy Fuels*, 2021, **5**, 4546

Recent advances in integrated CO_2 capture and utilization: a review

Shuzhuang Sun,[a] Hongman Sun,[b] Paul T. Williams*[c] and Chunfei Wu*[a]

CO_2 is one of the most important greenhouse gases leading to severe environmental issues. The increase of CO_2 emissions from the consumption of fossil fuels has received much research attention. One promising solution to reduce the impact of CO_2 is to integrate CO_2 capture and utilization (ICCU), which shows many advantages compared to traditional separate CO_2 capture and utilization (CCU) processes. The ICCU process shortens the path of CO_2 utilization such as CO_2 transportation and storage, and further negates the need for purification of products owing to the high conversion of CO_2. As an emerging integrated process, the improvement of ICCU performance is crucial for future applications. This review analyses and discusses the influence of the key process parameters of ICCU such as temperature, the presence of O_2 or H_2O in CO_2, GHSV *etc.*, to provide guidance for future investigation. The development and application of dual functional materials (DFMs) in ICCU are investigated and the roles and influence of interaction between adsorbents and catalysts are discussed. CaO showed superiority as an adsorbent to combine with CO_2 utilization catalysts owing to its low cost and high CO_2 capture capacity. The DFM system has opportunities to retard the deactivation of CaO owing to the presence of catalysts and the formed interaction. Nevertheless, there are several considerations from the industrial application perspective such as the reduction of overall cost and the possible post-processing requirements.

Received 25th May 2021
Accepted 20th July 2021

DOI: 10.1039/d1se00797a

rsc.li/sustainable-energy

1. Introduction

The significant increase of CO_2 emissions, from 280 ppm in 1760 to 410 ppm in 2020,[4] has become a serious global warming problem, resulting in a series of severe climate and environmental changes.[5] The emissions of CO_2 are mainly attributed to fossil fuel consumption,[6] in particular, the power generation sector emits the most CO_2, followed by industrial and transportation vehicles.[6,7] Therefore, there is an urgent requirement for CO_2 reduction which is recognised by the Intergovernmental Panel on Climate Change (IPCC) and the introduction of relevant policies and regulations.[8,9] The measures to reduce carbon emissions include the improvement of fuel energy efficiency,[10] CO_2 capture,[11,12] carbon storage[13,14] and CO_2 conversion.[15] CO_2 capture and storage (CCS) is a technology that decarbonises the use of fossil fuels in industries, such as power plants, steel works, cement kilns and oil refineries.[6] CCS includes three main stages: (1) CO_2 capture; (2) transportation; (3) permanent CO_2 storage by mineralizing[14] or injecting CO_2 into the ground or deep ocean.[7] Porous materials such as activated carbon and zeolites are possible adsorbents for carbon capture. However, the poor adsorption selectivity of physical carbon capture limits its industrial application. Chemical adsorption is more promising and has already been applied in the CO_2 capture process, mainly including aqueous monoethanolamine (MEA) adsorption[16] and calcium looping.[17] The captured CO_2 can be released at a high concentration by temperature swing. As for the storage process, CCS could also be combined with the current fossil fuel extraction processes, for example, the underground injection of CO_2 for crude oil enhanced oil recovery.[16,18] However, the high cost of separation, enrichment[19] and transportation of CO_2 (ref. 20) limits the deployment of CCS. Moreover, physical storage methods, such as underground or ocean injection, have negative impacts on natural ecology.[21] Therefore, in addition to the development of CCS, increasing attention is being paid to the application of the captured CO_2 as a feedstock to produce valuable chemicals or fuels.[2,22]

CO_2 capture and utilization (CCU) is a more sustainable process that can partially close the carbon cycle (as shown in Fig. 1). It is attractive to store the excess and uncertain supply of energy from renewable sources as stable chemical energy (*i.e.* methane, syngas or liquid chemicals[23,24]) by integrating with CCU.[25] Nowadays, there are many effective CO_2 utilization routes, including thermal-catalysis, photo-catalysis, electronic-catalysis,[26–28] plasma-catalysis,[29] *etc.* Several reviews have summarized integrated CO_2 capture and low-temperature utilization, such as the production of formic acid, carbamate, urea, [30,31] *etc.*, using MOFs/COFs or other chemicals.[15,31–33]

[a]School of Chemistry and Chemical Engineering, Queen's University Belfast, Belfast, BT7 1NN, UK. E-mail: c.wu@qub.ac.uk
[b]School of Science, State Key Laboratory of Heavy Oil Processing, China University of Petroleum, Qingdao, 266580, China
[c]School of Chemical and Process Engineering, University of Leeds, Leeds, LS2 9JT, UK. E-mail: p.t.williams@leeds.ac.uk

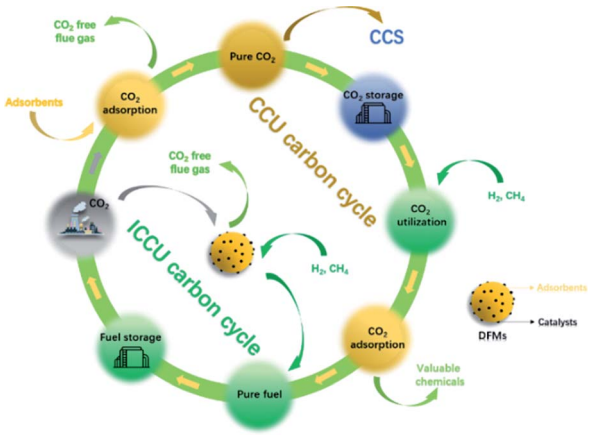

Fig. 1 Schematic diagram of ICCU and its advantages over traditional CCU and CCS processes.

However, considering the large scale application in industry, materials with high cost are not reasonable for reducing CO_2 emissions. This review focuses more attention on high-temperature CO_2 capture and *in situ* utilization technologies using low-cost adsorbents (*i.e.* MgO and CaO) and commonly used catalysts, such as Ni, Fe-based or low loading of noble metal-based materials. Although high-temperature applications will bring additional energy consumption, ICCU can be operated isothermally and continuously by swinging the inlet gas. Furthermore, rapid and efficient carbon capture can be achieved using low-cost CaO or MgO at high temperatures. Industrially applicable CO_2 hydrogenation can be easily realized using the most common catalysts (*i.e.* Ni, Fe or Cu-based catalysts). As an important C1 chemical, CO_2 has attracted much attention for various end-use applications including CO_2 methanation,[34,35] dry reforming of alkanes,[36,37] the reverse water-gas shift reaction,[38,39] *etc.*[15,31] However, CCU requires high CO_2 concentration for high conversion[40] and inevitable product purification before it can be utilized for the production of useful products. As shown in Fig. 1, the traditional CCU process includes several steps to achieve ideal carbon capture and utilization, and in which the process would be also accompanied by undesirable high costs.

In recent years, increasing studies have been carried out on integrated CO_2 capture and utilization (ICCU) to reduce the cost of the overall process by eliminating transportation and storage of CO_2. As shown in Fig. 1, ICCU achieves *in situ* CO_2 adsorption, separation and conversion using dual-function materials (DFMs), which consist of CO_2 adsorbents and catalysts. First, DFMs can capture CO_2 from flue gas (~15 vol% CO_2) to effectively reduce carbon emissions. When the carbon capture process is completed, the feed gas is switched to a reducing agent (*i.e.* H_2, CH_4) for the conversion of the adsorbed CO_2 accomplished with the regeneration of the adsorbents. The reduction of CO_2 in ICCU is carried out under reducing agent-rich conditions, further avoiding the purification of products by significantly improving the conversion of CO_2. Compared with the traditional MEA adsorption and calcium looping process, the ICCU process avoids CO_2 desorption by temperature swing, which is considered as an energy-intensive process. What's more, the effective *in situ* CO_2 utilization accompanied by adsorbent regeneration significantly simplifies the overall CO_2 utilization process.

The CO_2 adsorption, desorption and catalytic performances are significantly affected by the reaction temperature as well as the combination between catalysts and adsorbents. There are specific requirements for catalysts and adsorbents applied in DFMs, including the interaction between catalysts and adsorbents and the matching of adsorption/desorption efficiency and catalytic performance. ICCU has research gaps in both process optimization and catalytic mechanism investigation. In addition, the interactions and synergy effect between sorbents and catalysts of DFMs need significant research for better DFM design. This review critically introduces recent literature on CO_2 capture integrated with methanation, dry reforming of methane (DRM) and the reverse waste gas shift reaction (RWGS) from the perspectives of ICCU performance (*i.e.* CO_2 conversion, product yield, selectivity and process parameter optimization), CO_2 adsorbents (*i.e.* adsorbent system and understanding of the synergistic effect between catalysis and adsorption) and catalysts (*i.e.* catalytic system, active sites and catalytic mechanism). CO_2 utilization requires a specific reaction temperature which limits the selection and design of adsorbent in DFMs. In contrast, the presence of adsorbents promotes the performance of catalysts by assisting catalyst dispersion and provides close contact with CO_2 and catalysts. The interactions between adsorbents and catalysts are believed to play multifunctional roles in ICCU including promoting the stability of DFMs, providing effective catalytic sites and affecting the optimal parameters of ICCU. Furthermore, this review proposes research directions by pointing out the shortcomings of existing research from the perspective of industrial applications.

2. Progress in integrated CO_2 capture and methanation

Methane is the simplest hydrocarbon with the lowest C/H ratio, and is widely used in transportation, domestic heating and power plants because of its high calorific value (55.7 kJ g^{-1}), ready availability, low cost and clean combustion products. As shown in eqn (1), the conversion between CO_2 and CH_4, representing two important chemicals in C1 chemistry, has attracted great attention. Integrating CO_2 capture and methanation (ICCU-methanation) has advantages in improving the process and energy efficiency.

$$CO_2 + 4H_2 = CH_4 + 2H_2O \quad \Delta H_{298\ K} = -252.9\ \text{kJ mol}^{-1} \quad (1)$$

2.1 Influence of process parameters on ICCU-methanation

Temperature, reaction time, reducing agent parameters, the presence of O_2 and H_2O, *etc.*, have large influences on the efficiency of ICCU-methanation which normally happens at an intermediate temperature (~300 °C). Table 1 summarizes the

Table 1 The catalyst system, performance and reaction condition details of reported integrated CO_2 capture and methanation research work

DFMs	Adsorption process	Hydrogenation process	CO_2 cap.[a]	CO_2 con.[b]	CH_4 yield[c]	CH_4 sel.[d]	Cycle	Ref.
5% Ru,10% CaO/ γ-Al_2O_3	10% CO_2/N_2, 20 min, T = 320 °C, 1 atm	5% H_2/N_2, 20 min, T = 320 °C, 1 atm	0.4	82.7	0.30	NA	20 cycles	45
5% Ru,10% Na_2CO_3/γ-Al_2O_3	5% CO_2/N_2, 30 min, T = 320 °C, 1 atm	5% H_2/N_2, 30 min, T = 320 °C, 1 atm	0.5	NA	1.05	NA	3 cycles	46
5% Ru,10% CaO/ Al_2O_3 pellets	7.5% CO_2 + 15% H_2O + 4.5% O_2 + 73% N_2, 20 min, T = 320 °C, 1 atm	5% H_2/N_2, 60 min, T = 320 °C, 1 atm	0.14	91.2	0.13	NA	10 cycles	44
Commercial Ni catalyst/ hydrotalcite	15% CO_2/N_2, 100 ml min^{-1}, 1.34 atm, T = 350 °C	10% H_2/N_2, 100 ml min^{-1}, 1.34 atm, T = 350 °C	0.32	92	2.36 mol (kg^{-1} h^{-1})	NA	15 cycles	47
5% Ru,10% Na_2CO_3/Al_2O_3	7.5% CO_2 + 15% H_2O + 4.5% O_2/N_2, 300 ml min^{-1}, T = 320 °C, 1 atm	5% H_2/N_2, 300 ml min^{-1}, 30 min, T = 320 °C, 1 atm	0.29	73.3	0.21	NA	12 cycles	48
5% Ru,6.1% Na_2O/γ-Al_2O_3	7.5% CO_2 + 15% H_2O + 4.5% O_2/N_2, 15 min, GHSV = 521 h^{-1}, T = 300 °C, 1 atm	15% H_2/N_2, 15 min, GHSV = 1389 h^{-1}, T = 300 °C, 1 atm	0.44	80	0.35	NA	50 cycles	49
10% Ni,6.1% "Na_2O"/Al_2O_3	7.5% CO_2 + 15% H_2O + 4.5% O_2/N_2, 40 min, 30 ml min^{-1}, T = 320 °C	10% H_2/N_2, 60 min, 30 ml min^{-1}, T = 320 °C	0.43	71	0.30	NA		50
5% Ru,6.1% "Na_2O"/Al_2O_3	7.5% CO_2 + 15% H_2O + 4.5% O_2/N_2, 40 min 30 ml min^{-1}, T = 320 °C	10% H_2/N_2, 60 min, 30 ml min^{-1}, T = 320 °C	0.42	75	0.32	NA		
1% Ru,6.1% "Na_2O"/Al_2O_3	7.5% CO_2 + 15% H_2O + 4.5% O_2/N_2, 20 min, 100 ml min^{-1}, T = 320 °C, 1 atm	15% H_2/N_2, 200 ml min^{-1}, T = 320 °C	0.41	89	0.31	NA	20 cycles	51
1% Ru,10% Ni,6.1% "Na_2O"/ Al_2O_3	Same as above	Same as above	0.52	81	0.38	NA		
0.1% Ru,10% Ni, 6.1% "Na_2O"/ Al_2O_3	Same as above	Same as above	0.50	78	0.32	NA		
1% Pt, 10% Ni, 6.1% "Na_2O"/ Al_2O_3	Same as above	Same as above	0.35	87	0.25	NA		
0.1% Pt, 10% Ni, 6.1% "Na_2O"/ Al_2O_3	Same as above	Same as above	0.39	52	0.16	NA		
0.1% Pd, 10% Ni, 6.1% "Na_2O"/ Al_2O_3	Same as above	Same as above	0.47	57	0.18	NA		
$Ru_{10}Na_2CO_3$	11% CO_2/Ar, 1 min, 1200 ml min^{-1}, T = 400 °C 1 atm	10% H_2/Ar, 2 min, 1200 ml min^{-1}, T = 400 °C, 1 atm	0.42	94	0.39	>99		52
$Ru_{10}CaO$	Same as above	Same as above	0.34	80	0.27	>99		
10% Ni/CaO	10% CO_2 + 10% H_2O + 80% N_2, 120 min, 40 ml min^{-1}, T = 500 °C, 1 atm	90% H_2/N_2, 230 min, 40 ml min^{-1}, T = 500 °C, 1 atm	8.96	93	8.34	93	5 cycles	43
10% Ni/CaO	10% CO_2 + 10% H_2O + 80% N_2, 120 min, 40 ml min^{-1}, T = 600 °C, 1 atm	90% H_2/N_2, 230 min, 40 ml min^{-1}, T = 600 °C, 1 atm	15.49	96	14.94	96	NA	
10% Ni/CaO	10% CO_2 + 10% H_2O + 80% N_2, 120 min, 40 ml min^{-1}, T = 700 °C, 1 atm	90% H_2/N_2, 230 min, 40 ml min^{-1}, T = 700 °C, 1 atm	16.22	83	4.7	29	NA	
15% Ni 15% CaO/Al_2O_3	10% CO_2/Ar, 1 min, 1200 ml min^{-1}, T = 520 °C, 1 atm	10% H_2/Ar, 2 min, 1200 ml min^{-1}, T = 520 °C, 1 atm	0.16	88	0.14	87		41
15% Ni 15% Na_2CO_3/Al_2O_3	10% CO_2/Ar, 1 min, 1200 ml min^{-1}, T = 400 °C, 1 atm	10% H_2/Ar, 2 min, 1200 ml min^{-1}, T = 400 °C, 1 atm	0.21	88	0.19	86		

Table 1 (*Contd.*)

DFMs	Adsorption process	Hydrogenation process	CO_2 cap.[a]	CO_2 con.[b]	CH_4 yield[c]	CH_4 sel.[d]	Cycle	Ref.
2D-layered Ni–MgO–Al_2O_3, 2.0NiMgAl-LDO-re	15% CO_2/N_2, 25 s, 70 ml min^{-1}, $T = 250$ °C, 1 atm	100% H_2, 35 s, 70 ml min^{-1}, $T = 250$ °C, 1 atm	0.32	100	NA	100	10 cycles	42
1% Ni/CeO_2–CaO-physically mixed	15% CO_2/N_2, 60 min, 50 ml min^{-1}, $T = 550$ °C, 1 atm	100% H_2, 60 min, 50 ml min^{-1}, $T = 550$ °C, 1 atm	15.3	62	8.0	84		53
5% Ru/CeO_2–MgO	65% CO_2/N_2, 60 min, 50 ml min^{-1}, $T = 300$ °C, 1 atm	5% H_2/N_2, 60 min, 50 ml min^{-1}, $T = 300$ °C, 1 atm	4.25	79	3.36	NA	10 cycles	54

[a] CO_2 capture capacity (mmol g_{DFM}^{-1}). [b] CO_2 conversion (%). [c] CH_4 yield (mmol g_{DFM}^{-1}). [d] CH_4 selectivity (%).

performance of ICCU-methanation in relation to catalyst systems and reaction conditions. Most of those reported in the literature have been carried out under isothermal conditions and atmospheric pressure.

Temperature is one of the most important parameters in catalytic processes. For ICCU-methanation, Bermejo-López *et al.*[41] investigated the influence of a wide temperature range, *i.e.* 200–600 °C, on ICCU-methanation using Ni–Ca/Al_2O_3 DFMs. The temperature showed a positive correlation with CO_2 capture capacity, CH_4 yield and CO yield. A similar trend of temperature related to CO_2 capture capacity was observed by Zhou *et al.*[42] and Jo *et al.*[43] The matching of temperature between adsorption and methanation is also very important for ICCU. Generally, lower process temperature promotes CH_4 selectivity but decreases CO_2 conversion for ICCU-methanation. By comparing different temperatures (280–350 °C), Zheng *et al.*[44] achieved the best ICCU performance at 320 °C (32.41 ml CO_2 captured and 31.56 ml CH_4 generated). A higher temperature was found to decrease the CO_2 capture capacity and cause excessive oxidation of Ru for the processing of O_2-containing flue gas (32.86 ml CO_2 captured and 29.73 ml CH_4 generated at 350 °C), while a lower temperature significantly limited the catalytic activity (41.21 ml CO_2 captured and 1.2 ml CH_4 generated at 280 °C).

In addition to the effect of temperature, the reaction time of adsorption and conversion stages also affects the catalytic performance. Zheng *et al.*[44] investigated the influence of adsorption time on ICCU-methanation. Increasing the reaction time of adsorption benefited the generation of CH_4. However, it was found that the CO_2 adsorption rate dropped significantly after 20 min. In addition, a longer adsorption time resulted in the deactivation of catalysts by inducing excessive oxidation of catalysts in the flue gas. As listed in Table 1, most of the research used more than 20 min reaction time in the first carbon capture stage. This could increase the overall CO_2 capture capacity. However, it might not be beneficial to the overall ICCU-methanation process. Excessive CO_2 adsorption could produce more carbonates than active formate species which are mainly responsible for the formation of methane. For example, Zhou *et al.*[42] applied a fast adsorption and methanation process (25 s and 35 s for adsorption and methanation) and reported a nearly 100% CO_2 conversion. This was due to the formation of dominant formate species and few carbonates.

The concentration of H_2 is another important parameter that has a significant impact on CH_4 yield. Wang *et al.*[48] investigated the influence of H_2 partial pressure (5% and 10% H_2/N_2) and found that the presence of more sufficient H_2 could generate more CH_4 (58.66 ml and 131 ml CH_4). The authors reported that a higher H_2 concentration is important for the activation of Ru-based DFMs when processing O_2-containing flue gas. A higher H_2 concentration could also effectively improve the CO_2 conversion by positively promoting the equilibrium of CO_2 methanation.[43,53] Apart from the gas concentration, GHSV also influences the ICCU performance by altering the gas diffusion pathways within DFMs.[44] Generally, a higher GHSV results in an enhanced CO_2 conversion and is accomplished with higher H_2 consumption.

In practice, it is known that contaminants in flue gas such as H_2O and O_2 can affect CO_2 capture[55] and conversion.[56] Martha *et al.*[50] simulated a flue gas by mixing 4.5% O_2 and 15% H_2O with 7.5% CO_2/N_2 to investigate CH_4 formation using Ni-based DFMs. The reduction of ICCU performance in relation to CH_4 production was observed owing to the oxidation of active metals. In addition, the presence of H_2O and O_2 in the feed gas decreases the capacity of CO_2 capture by competitive adsorption.[44] Interestingly, the presence of H_2O might not always play a negative role in ICCU. Miguel *et al.*[47] found that H_2O can participate in CO_2 desorption, removing CO_2 and promoting CH_4 formation. The presence of H_2O helped to dissolute K_2CO_3, which promoted the formation of bidentate carbonate in the CO_2 adsorption process. The H_2O generated in CO_2 methanation was also suggested to be helpful for CO_2 desorption, especially in the regeneration of sorbent sites.[47]

2.2 Development of DFMs for ICCU-methanation

2.2.1 Adsorbents in DFMs for ICCU-methanation. In this section, the role of sorbents in DFMs is reviewed and discussed for ICCU-methanation. As shown in Table 1 and Fig. 2, Na_2O, K_2O, MgO and CaO are the most common sorbents for this process. CaO is widely used as a CO_2 adsorbent owing to its

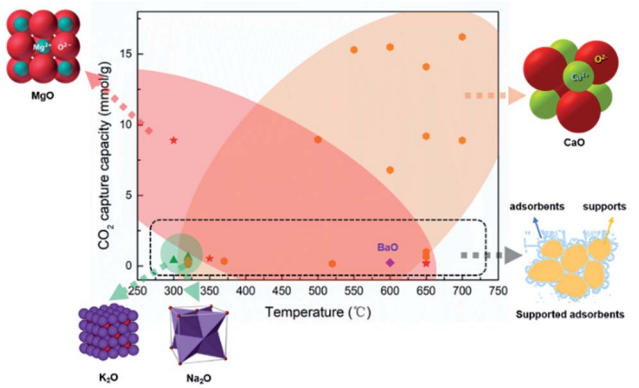

Fig. 2 Summary of the CO_2 adsorption capacity of DFMs applied in ICCU.[41–54]. (orange zone: CaO application in ICCU; red zone: MgO application in ICCU; green zone: K_2O and Na_2O application in ICCU; black dotted zone: supported adsorbent application in ICCU).

excellent theoretical adsorption capacity and low price. Due to sintering caused by volume change during the transformation between CaO and $CaCO_3$, highly dispersed CaO could provide better stability than limestone derived CaO. Melis *et al.*[45] dispersed CaO onto γ-Al_2O_3 and reported an increased CH_4 yield, demonstrating that the spillover of CO_2 from CaO to active sites occurred within DFMs. Due to the temperature limitation of CO_2 methanation, Na_2O and K_2O are also popular for ICCU-CO_2 methanation. Martha *et al.*[50] studied dispersed alkaline adsorbents, including Na_2O, CaO, K_2O and MgO, and obtained enhanced methanation performance using Na_2O and CaO (0.614, 0.610, 0.466 and 0.213 $mmol_{CH_4}$ g_{DFM}^{-1} for Na_2O, CaO, K_2O and MgO, respectively). The doping of Na in γ-Al_2O_3 promotes the formation of Al–O^- sites by promoting the formation of reversible bidentate and polydentate carbonates.[57] Mertha *et al.*[50] found that Na_2O showed the fastest kinetics towards CH_4 production compared to CaO, K_2O and MgO. In addition, the Na_2CO_3-based DFMs showed acceptable stability (*i.e.* 27% decrease after 10 cycles) and the adsorption performance could be maintained by increasing the reduction time.[48] The adsorption capacity of different alkali metal species varies as well. Bermejo-López *et al.*[52] investigated oxides (CaO or Na_2O) and hydrated oxides ($Ca(OH)_2$ or NaOH) as CO_2 storage sites, and reported that the former oxides were more reactive for CO_2 adsorption.

Mg-based adsorbents are widely used in DFMs due to their low cost and medium adsorption temperature (~300 °C), as shown in Table 1 and Fig. 2. In addition, MgO does not have serious sintering issues like CaO, and the use of adsorbent carriers can be avoided to achieve more abundant adsorption capacity. Miguel *et al.*[47] investigated the cycle stability of a Mg–Al hydrotalcite-based DFM. The authors obtained a decreased CO_2 capacity in cycles, from 0.52 mmol g^{-1} to 0.32 mmol g^{-1}, owing to the formation of irreversible bulk polydentate carbonate from unidentate and bridged carbonates. Thus promoters such as Li were used to stabilize MgO during the carbon capture stage of ICCU. Sun *et al.*[54] applied alkali metal (Li, Na, and K) promoted MgO in DFMs and obtained ~4 mmol g_{DFM}^{-1} CO_2 capacity after 10 cycles at a temperature below 300 °C. Attractively, Zhou *et al.*[42] synthesized 2D-layered Ni–MgO–Al_2O_3 nano-sheets and obtained prolonged cycling performance at low temperatures (≤250 °C). However, the formation of difficult-to-reduce species, such as Ni–O–Mg and/or Ni–O–Al, suppressed the reducibility of low Ni-loading catalysts. Zhou *et al.*[42] observed the formation of formate species in the CO_2 capture process, which was formed from the hydrogenation of carbonate and/or bicarbonate.[58] These formed formate species are desirable for methanation.[59]

The loading of adsorbents in DFMs can directly affect the capacity of CO_2 capture. Melis *et al.*[46] reported a positive correlation between adsorbent loading and CO_2 capture capacity using dispersed K_2CO_3 as an adsorbent. However, a higher loading of the adsorbent could not always result in a better CO_2 capture capacity when applying other alkali metal-based adsorbents. Melis *et al.*[46] found an optimal loading of 10% for Na_2CO_3 and MgO. In addition to providing adsorption sites, the presence of sorbent could also promote catalytic performance in relation to the conversion of CO_2. For example, Bermejo-López *et al.*[52] reported that the dispersion of Ru or Ni was improved with the increase of adsorbent loading.

Different adsorbents show various performances for the process temperature of ICCU-methanation. Bermejo-López *et al.*[52] observed that the performance of the CaO-based DFMs showed a significantly more positive correlation with the increase of temperature, while the medium temperature (*i.e.* 340 °C) is optimal for the Na_2CO_3-based DFMs. In the case of using CaO, a higher temperature was attributed to the decomposition of stable carbonates, while the Na_2CO_3 sorbent could release CO_2 at a relatively lower temperature. The CaO and Na_2CO_3-based DFMs with low adsorbent loadings (*i.e.* 5 wt%) possess relatively weak basicity, results in decreased CO_2 storage capacity and CH_4 production at higher temperature.

In addition, the carriers used to disperse the adsorbent affect the adsorption performance in ICCU-methanation. For example, Martha *et al.*[50] studied carrier materials, including CeO_2, CeO_2/ZrO_2, Nazeolite-X, H-mordenite zeolite, SiC, SiO_2 and ZrO_2–Y and demonstrated that γ-Al_2O_3 was the most suitable carrier for DFMs. In addition to acting as a carrier, γ-Al_2O_3 could adsorb CO_2 over Al_2O_3–OH groups.[59] Laura et al.[59] proposed that Al–O^-–Na^+ species formed by the interaction between Na_2O and Al_2O_3 allowed CO_2 adsorption by the formation of bidentate carbonates over the sorbent surface using *in situ* DRIFTS (diffuse reflectance infrared fourier transform Spectroscopy) characterization.

As shown in Fig. 2, sorbents for CO_2 capture could be dispersed into supports to enhance the stability of adsorbents, however, it could significantly reduce the capacity of CO_2 capture owing to the reduction of adsorbent content. It is important to develop intermediate temperature adsorbents (~300 °C) with excellent stability and CO_2 capture capacity for ICCU-methanation to increase the CO_2 throughput of DFMs.

2.2.2 Catalysts in DFMs for ICCU-methanation. The role of catalytic sites in DFMs for ICCU-methanation is discussed in this section. It is known that the reduction of CO_2 to CH_4 is an eight-electron complicated process with significant kinetic

limitations.[60] Therefore, CO_2 methanation requires suitable catalysts to achieve acceptable activity and selectivity. Metal-based catalysts, such as Ni, Ru and Rh, have been widely investigated for this process. As shown in Table 1, Ni was chosen as the methanation catalytic site by many researchers due to its high catalytic activity and relatively low cost. The effect of Ni loading in DFMs on ICCU-methanation was studied by Bermejo-López *et al.*[41] In general, higher Ni loading promotes CO_2 capture and CH_4 generation owing to the closer contact between the adsorbents and metallic phase. Furthermore, increasing Ni loading could also slightly promote the decomposition of carbonates at lower temperatures.

Notably, the interaction between catalysts and adsorbents could positively affect ICCU-methanation. It was proposed that the reducibility of Ni species was enhanced in the presence of the adsorbent.[41] The adsorbent impeded the close contact between Ni and Al_2O_3 weakening the interaction between both phases and favoring the formation of reducible NiO species.

However, there are shortcomings of Ni-based catalysts in DFMs for ICCU-methanation. When processing O_2-containing flue gas, Ni-based catalysts were oxidized and required much higher temperatures (*i.e.* 600 °C) to reduce.[51] Other possible causes of the deactivation of Ni-based catalysts at low temperatures are the interaction of the metal particles with CO and the formation of mobile Ni subcarbonyls.[61] Introducing other metals could help to decrease the reduction temperature of oxidized Ni-based DFMs in the step of CO_2 methanation. For example, Martha *et al.*[51] introduced noble metals (Pt, Pb or Ru ≤ 1%) into Ni-based DFMs and obtained enhanced ICCU performance in the presence of H_2O and O_2. The authors[51] also reported stable capacity of CO_2 capture (0.52 mmol g_{cat}^{-1}) and CH_4 yield (0.38 mmol g_{cat}^{-1}) after 20 cycles of capture and methanation using 1% Ru, 10% Ni, and 6.1%Na_2O/Al_2O_3 at 320 °C, indicating excellent long term stability of the Ru-promoted Ni-based DFM.

Noble metals could not only be used as a promoter of Ni-based DFMs, but also show impressive catalytic performance as the main active metal. Ru was the most promising one owing to its excellent catalytic activity of CO_2 methanation. Melis *et al.*[45] applied 5 wt% Ru/CaO/γ-Al_2O_3 DFMs in ICCU-methanation and obtained around 290 μmol g_{cat}^{-1} CH_4 yield. Sun *et al.*[54] utilized 10 wt% Ru/CeO_2–MgO and achieved higher CH_4 yield (7.07 mmol g_{cat}^{-1}) and CO_2 conversion (89%) in ICCU-methanation. Ru-based DFMs have also shown excellent stable performance in ICCU. Wang *et al.*[49] applied 5% Ru-6.1% Na_2O/γ-Al_2O_3 DFMs and obtained 0.35 mmol g_{cat}^{-1} CH_4 yield after 80 h operation. During the stability test, there was no loss of the BET surface area, CO_2 capture capacity and Ru dispersion. Ru showed acceptable performance in the presence of O_2. For example, Zheng *et al.*[44] investigated the performance of Ru–CaO/Al_2O_3 DFMs under simulated flue gas conditions and proposed that Ru-based catalysts could be easily reduced after exposure to O_2-containing CO_2 flue gas. As shown in Fig. 3a, it is suggested that H_2 reduced oxidized Ru first, followed by the spillover of CO_2 from CaO to Ru. Lastly, the dissolved CO_2 at Ru sites formed CH_4 with the assistance of H_2.

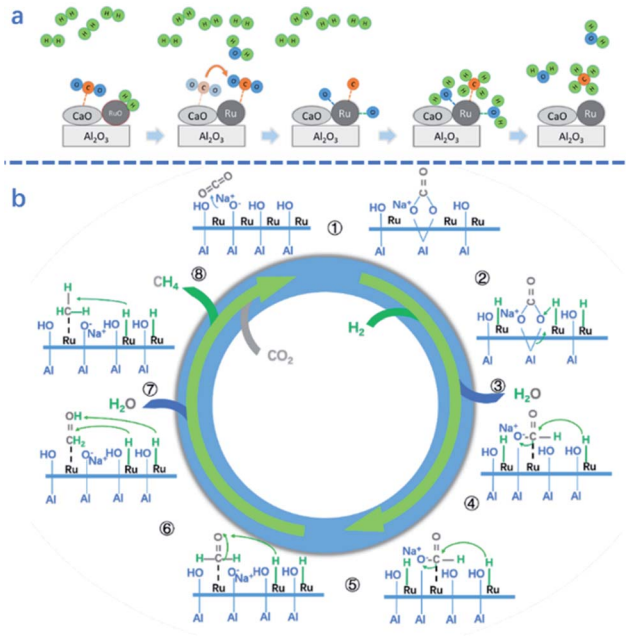

Fig. 3 (a) Proposed schematic mechanism of the surface reactions on Ru,CaO/Al_2O_3 DFMs for CO_2 methanation in ICCU.[44] (b) Proposed CO_2 methanation mechanism over 5%Ru–Na_2O/Al_2O_3 DFMs.[59]

It is known that the loading of Ru is closely related to the catalytic performance. Bermejo-López *et al.*[52] proposed that a higher Ru loading in Ru–10%Na_2CO_3/Al_2O_3 resulted in an acceptable ICCU performance even at a notably lower temperature (*i.e.* 310 °C). However, there is an optimum Ru loading for ICCU-methanation. For example, Sun *et al.*[54] reported that 10% Ru/CeO_2–MgO showed poorer stability than 5% Ru/CeO_2–MgO. It is mainly attributed to the presence of more oxygen vacancies that remained in 5% Ru/CeO_2–MgO. Better dispersion of Ru also promotes ICCU-methanation. For example, Melis *et al.*[45] reported that increasing the weight ratio of CaO to Ru promoted CO_2 spillover from CaO to Ru sites and then increased the performance of ICCU-methanation.

The distance between the active metals and the adsorbents also affects the performance of ICCU-methanation. Melis *et al.*[45] compared physically mixed 10% Ru/γ-Al_2O_3 and 10% CaO/γ-Al_2O_3 with 10% Ru-10% CaO/γ-Al_2O_3 for ICCU-methanation. The physically mixed DFMs showed a poor ICCU performance (0.12 g-mol CH_4/kg DFM) owing to the longer distance between active sites within the DFMs decreasing the effective CO_2 spillover. However, Sun *et al.*[53] reported different conclusions by comparing physically mixed Ni/CeO_2–CaO with impregnated Ni/CeCaO DFMs. The longer distance between Ni and CaO prevented the coverage of Ni from the formation of $CaCO_3$. Furthermore, the introduction of a CeO_2 support would promote the dispersion of Ni and increase the performance of ICCU-methanation.

The addition of additives could promote the catalytic performance of DFMs for ICCU-methanation. For example, Stefano *et al.*[62] introduced various alkali metals (Li, Na, and K carbonates *vs.* nitrates) into 1% Ru/Al_2O_3 DFMs and found that

both the capture capacity of CO_2 and activity of methanation were enhanced *via* doping with Li (nitrates), which could react with Al_2O_3 to form a mixed spinel phase.

Investigating the catalytic mechanism helps to develop DFMs for ICCU-methanation. The mechanism and key intermediates of CH_4 formation from the ICCU process were studied by *in situ* diffuse reflectance infrared fourier transform spectroscopy (DRIFTS).[59] Proaño *et al.*[59] investigated the two steps of ICCU-methanation, including CO_2 adsorption and hydrogenation, over 5% Ru–6.1% Na_2O/Al_2O_3 DFMs. The authors found that CO_2 absorbed on the AlO^-–Na^+ species formed bidentate carbonates (*i.e.* 1st step in Fig. 3b), and then the adsorbed bicarbonates and bidentate carbonates spilled over onto the Ru-support interface during the CO_2 methanation process, with formates as reaction intermediates (*i.e.* 2nd and 3rd steps in Fig. 3b), which is consistent with the results reported by Sun *et al.*[54] In addition to the adsorbent, Ru as the catalytic site also showed the capacity of CO_2 adsorption,[44,59] generating carbonyl groups.[54]

A lot of research has been conducted on the production of CH_4 by ICCU, but there is no valuable economic evaluation research in this field yet. However, ICCU-methanation can be combined with renewable H_2, and it still has a very broad prospect as integrated hydrogen storage and carbon-neutral solution.

3. Progress in integrated CO_2 capture and DRM

Compared to CO_2, the greenhouse effect of CH_4 is 22 times higher. Currently, CH_4 is widely used to produce H_2 by chemical looping reforming[63] or steam methane reforming.[64] Dry reforming of methane (DRM) utilizing these two major greenhouse gases, as shown in eqn (2), has received increasing attention in recent years.[36,65] In addition to CH_4, C_2H_6 and other low-carbon alkanes could also be used for dry reforming. Integrated CO_2 capture and dry reforming (ICCU-DRM) provides a promising solution for utilizing low carbon alkanes accompanied by the reduction of CO_2 emissions. Synthesizing liquid fuels or high-value hydrocarbons by Fischer–Tropsch synthesis using the products from the ICCU-DRM process could be a practical route for upgrading alkanes.

$$CH_4 + CO_2 = 2CO + 2H_2 \quad \Delta H_{298\ K} = +247\ kJ\ mol^{-1} \qquad (2)$$

3.1 Influence of process parameters on ICCU-DRM

In this section, the influences of process parameters on the performance of ICCU-DRM are reviewed and discussed. As shown in Fig. 4a, there are various side reactions in ICCU-DRM, including CH_4 decomposition and the reverse-water-gas shift reaction (RWGS), which would generate coke on the surface of DFMs and affect the ratio of H_2/CO in the final product.

Temperature is one of the most effective parameters to influence the balance of DRM and side reactions. Molina-Ramírez *et al.*[66] studied different temperatures (600–700 °C) of ICCU-DRM using a non-supported Ni–Ba bifunctional catalyst. The conversion of CH_4 increased with the increase of temperature (11.04% at 600 °C and 18.57% at 700 °C), while the selectivity to CO showed an opposite trend (14.89% at 600 °C and 4.69% at 700 °C). The side reactions, especially CH_4 decomposition, are favored at a higher temperature. The ratio of H_2/CO increased from 5.7 at 600 °C to 20.4 at 700 °C, which was accompanied by a significant carbon deposition on the surface of the DFMs. By applying dry reforming of ethane, Ahmed *et al.*[67] investigated the influence of reaction temperature on Ni_{20}@$(K–Ca)_{50}/(\gamma\text{-}Al_2O_3)_{50}$ over ICCU and found that the yield of syngas continuously increased with increasing temperature. Ethane conversion was positively correlated with temperature and could be fully converted at a higher

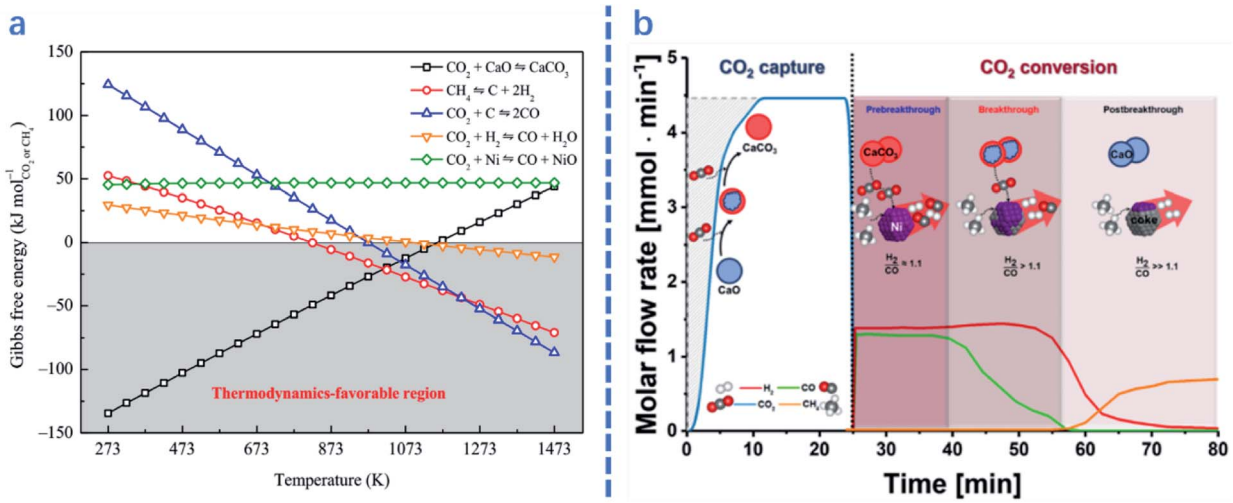

Fig. 4 (a)Gibbs free energy of related reactions in integrated CO_2 capture and DRM as a function of temperature.[2] (b) Coupled CO_2 capture and conversion reactions: molar flow rate of the effluent gas in the first cycle of the coupled CO_2 capture–conversion process and schematic description of the main processes occurring in the reactor.[1]

temperature (>650 °C), while the CO_2 conversion equilibrated at ~65% (>600 °C).

For ICCU-DRM, a higher temperature is not always preferred. Molina-Ramírez *et al.*[66] reported that the optimal temperature of Ni–Ba DFMs for CO_2 adsorption is 650 °C (0.37 mmol g^{-1}), capturing 0.23 and 0.13 mmol g^{-1} CO_2 at 600 and 700 °C, respectively. It is suggested that a higher temperature enables the adsorption to approach equilibrium faster, but reduces the adsorption capacity at equilibrium. In terms of the desorption temperature for ICCU-DRM, Kim *et al.*[1] proposed that a reaction temperature of around 720 °C could steadily release CO_2. Too fast desorption would cause excessive CO_2 release at the initial time of the conversion stage, while slow desorption would decrease the overall efficiency of ICCU-DRM.

Reaction time is another important parameter in ICCU-DRM. For example, Kim *et al.*[1] studied different stages of ICCU through continuous online gas analysis. As shown in Fig. 4b, three reaction stages were proposed: (1) in the pre-breakthrough stage, CO_2 and CH_4 were almost fully converted, only 0.08% and 0.06% escaped, respectively. The produced syngas had a slightly higher H_2/CO ratio (~1.06 : 1) than thermodynamic equilibrium (0.94 : 1) at 720 °C, probably owing to the decomposition of CH_4. (2) The CO yield was gradually decreased due to the reduction of CO_2 release, while the H_2 yield remained stable during the following ~18 min, namely the breakthrough stage. (3) The H_2 mole flow rate gradually decreased in the post-breakthrough stage due to the deactivation of the catalyst, which was caused by the deposition of carbon generated by CH_4 decomposition in the previous stages. Therefore, the ratio of H_2/CO in the product can be controlled by adjusting the reaction time at different stages of ICCU-DRM.

3.2 Development progress of DFMs for ICCU-DRM

3.2.1 Adsorbents in DFMs for ICCU-DRM. The current CO_2 adsorbents applied in ICCU-DRM are mainly alkali metal oxides. High-temperature adsorbents, especially CaO-based materials, are the most commonly applied adsorbents owing to the thermodynamic requirements of DRM. However, the sintering of CaO is the most severe problem in this process. Kim *et al.*[1] applied CaO as the adsorbent and observed a significant decrease of CO_2 capture capacity after several cycles of ICCU-DRM. What's more, the sintering of CaO would shorten the pre-breakthrough stage, as shown in Fig. 4b and 5a, which was suggested as the best stage for ICCU-DRM.

The presence of catalysts also affects the performance of adsorbents in ICCU-DRM. As shown in Fig. 5b, Tian *et al.*[2] reported that introducing catalysts in adsorbents significantly promoted the decomposition of $CaCO_3$ (~3 times faster). A similar promotion effect of catalysts on adsorbents was also reported by Ahmed *et al.*[67]

Other adsorbents were also applied in ICCU-DRM, however with poor adsorption performance. For example, Molina-Ramírez *et al.*[66] synthesized a Ni–Ba unsupported DFM and obtained 0.232 mmol g^{-1} capacity of CO_2 capture. In addition, MgO is not a suitable adsorbent for ICCU-DRM as Ahmed *et al.*[67] only achieved 0.22 mmol g^{-1} capture capacity of CO_2 using $Ni_{10}@(K–Mg)_{25}/(\gamma\text{-}Al_2O_3)_{75}$ DFMs at 650 °C, which was much lower than that achieved by Ca-based adsorbents.

3.2.2. Catalysts in DFMs for ICCU-DRM. As DRM requires a large amount of energy to process owing to its thermodynamic properties,[68] the introduction of catalysts such as Ni, Ru, Mo or Co-based catalysts can reduce the thermodynamic barrier and reduce the reaction temperature. The interaction between metals and adsorbents plays a key role in the ICCU-DRM process. Tian *et al.*[2] investigated two NiO forms in CaO–Ni bifunctional sorbent-catalysts by XPS and H_2-TPR. The proportion of interacted NiO increased from 64.0 to 80.7 atomic % with the increase of the Ca/Ni ratio. It was suggested that the presence of interacted NiO enhanced the ICCU-DRM. The authors also proposed that the sintering of catalysts could be prohibited by strengthening the metal–support interaction and/or the confinement effect of the support in the material matrix.

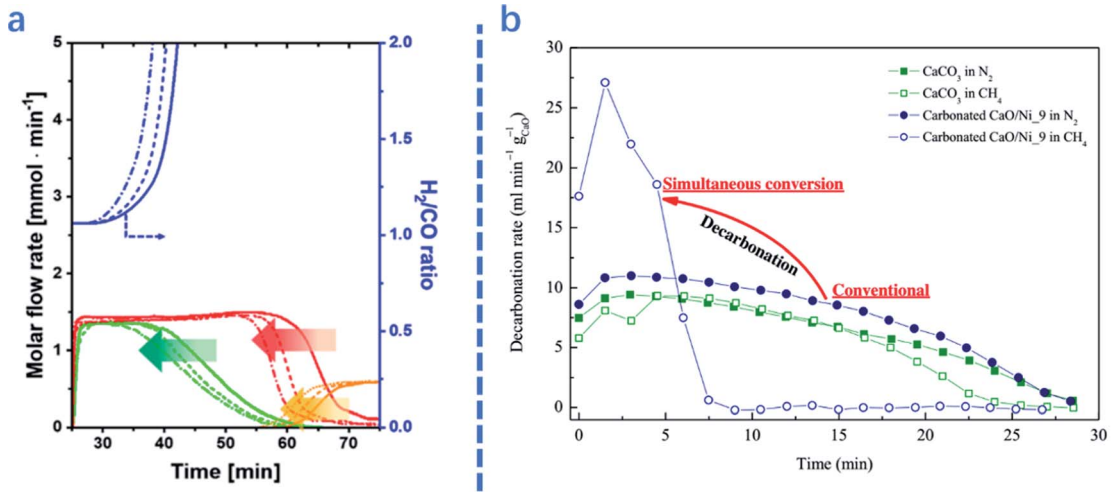

Fig. 5 (a): Molar flow rate and H_2/CO ratio of the effluent gas as a function of cycle number: (—) 1st, (- - -) 5th, and (–•–) 10th cycles. The arrows highlight the trends with cycle number;[1] (b) comparison of decarbonation kinetics as a function of time at 1073 K between CaL methane reforming and separate CaL processes.[2]

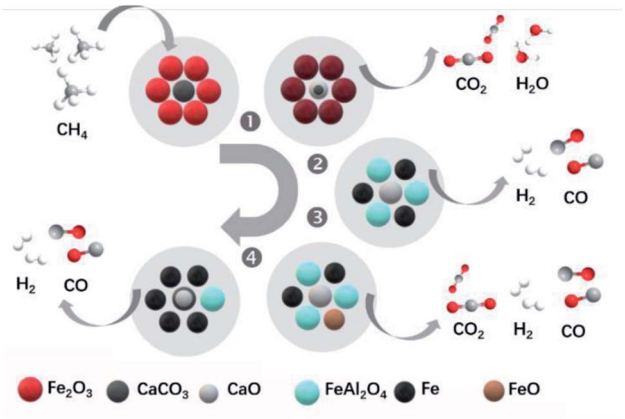

Fig. 6 Diagram of the reaction mechanism for the novel Ca–Fe chemicallooping reforming process.[3]

Fe-based catalysts also showed a good performance for ICCU-DRM. For example, Zhao *et al.*[3] demonstrated a Ca–Fe chemical looping reforming process for ICCU. The authors observed the occurrence of the reaction between CH_4 and $CaCO_3$ and Fe_2O_3. As shown in Fig. 6b, in the 1st stage, the rapid full CH_4 oxidation reaction occurred and all Fe_2O_3 was changed into Fe_3O_4 (eqn (3) and eqn (4)) without CO generation.

In the 2nd stage, the interaction between Fe-based oxygen storage materials and CO_2 adsorbents accompanied by the CH_4 reforming of $CaCO_3$ (eqn (5) and eqn (6)) achieved pure syngas production. Fe_3O_4 was gradually transformed into Fe and $FeAl_2O_4$ with the grain size change in this stage. Along with further interactions, FeO rather than Fe was detected at the 3rd reaction stage. This might be attributed to the influence of the oxygen sources, including CO_2, lattice oxygen from the incompletely reduced Fe-based oxygen storage materials, or even lattice oxygen from the Al_2O_3 support. In the final stage, there was a reappearance of $CaCO_3$, which suggested that when the spine $FeAl_2O_4$ was reformed by methane, the unwanted byproduct CO_2 was recaptured by the carbonation reaction and thus utilized. In conclusion, the Ca–Fe DFM could restore its state and activity after oxidation and carbonation in flue gas and showed acceptable cycle stability.

$$12Fe_2O_3 + CH_4 \rightarrow 8Fe_3O_4 + CO_2 + 2H_2O \quad \Delta G_{1173\ K} = -532.33\ kJ\ mol^{-1} \quad (3)$$

$$6Fe_2O_3 + CH_4 \rightarrow 4Fe_3O_4 + CO_2 + 2H_2 \quad \Delta G_{1173\ K} = -300.08\ kJ\ mol^{-1} \quad (4)$$

$$CaCO_3 + CH_4 \rightarrow CaO + 2CO + 2H_2 \quad \Delta G_{1173\ K} = -74.96\ kJ\ mol^{-1} \quad (5)$$

$$3CaCO_3 + CH_4 \rightarrow 3CaO + 4CO + 2H_2O \quad \Delta G_{1173\ K} = -84.07\ kJ\ mol^{-1} \quad (6)$$

Introducing specific additives promotes ICCU-DRM. Ahmed *et al.*[67] proposed that a K-introduced DFM showed better reducibility than a Na-introduced DFM by enhancing catalyst–support interactions. The promotion effect of Ni–Ca interactions was also verified by comparison with that of Ni–Mg DFMs. It was noted that with the introduction of alkaline metals, the ratio of H_2/CO was affected. For example, the K-introduced DFM showed a higher H_2/CO ratio owing to the higher conversion of dry reforming ethane and other side reactions.

4. Progress in integrated CO_2 capture and RWGS

The reverse water gas shift (RWGS) reaction is another important reaction in C1-chemistry, which can connect with the production of valuable hydrocarbons through Fischer–Tropsch using the produced syngas.[69,70] As shown in eqn (7), the RWGS reaction is an endothermic process with lower Gibbs energy than DRM. Although more expensive H_2 is used, the RWGS process has fewer side reactions than DRM. The integrated CO_2 capture and RWGS (ICCU-RWGS) process possesses the potential opportunity to directly produce pure syngas from flue gas.

$$CO_2 + H_2 = CO + H_2O \quad \Delta H_{298\ K} = +41.2\ kJ\ mol^{-1} \quad (7)$$

4.1 Influence of process parameters on ICCU-RWGS

In this section, several key parameters, including temperature, CO_2 concentration and the presence of contaminants, are reviewed for ICCU-RWGS. As shown in Fig. 7b, Luis *et al.*[71] reported that a higher temperature improved both CO_2 conversion and CO selectivity owing to the endothermic properties of

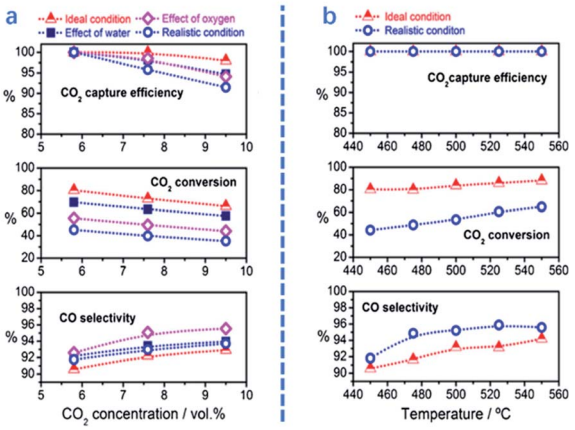

Fig. 7 CO_2 capture efficiency, CO_2 conversion, and CO selectivity as a function of (a) CO_2 concentration (5.8–9.5%) at 450 °C and (b) reaction temperature with 5.8% CO_2. The gas composition–capture phase: CO_2 diluted in nitrogen (ideal condition), CO_2 diluted in nitrogen saturated with 4% of water vapour (effect of water), CO_2 diluted in nitrogen with 4% of oxygen (effect of oxygen) and CO_2 diluted in nitrogen with 5% of oxygen and 4% of water (realistic condition). Gas hourly space velocity (GHSV)-1620 ml g_{cat}^{-1} h^{-1}. Reduction phase: Pure hydrogen with a GHSV of 3900 ml g_{cat}^{-1} h^{-1}. The CCR period length was 215 s, *i.e.* 107.5 s for the CO_2 capture and reduction phase.[71]

RWGS. A similar trend in relation to the influence of temperature was also reported by Jo *et al.*[43] using Ni/CaO DFMs. Shao *et al.*[72] analyzed the temperature-programmed desorption of ICCU-RWGS using a $Fe_xCo_yMg_{10}CaO$ DFM and found that CO could be generated at 550 °C, which was earlier than CO_2 release. Within a certain temperature range (<650 °C), operating ICCU-RWGS at a higher temperature could generate more CO due to the release of more CO_2. However, too fast CO_2 release rate at high temperatures could reduce its conversion to CO.

O_2 and H_2O are present in flue gas and affect the performance of ICCU-RWGS. Luis *et al.*[71] investigated the influence of the presence of O_2 or H_2O on ICCU-RWGS using FeCrCu/K/hydrotalcite DFMs (Fig. 7a). The realistic conditions resulted in a poorer ICCU-RWGS performance owing to the deactivation of active sites (*e.g.* by surface oxidation or adsorption). The presence of H_2O could suppress ICCU-RWGS by competitively adsorbing CO_2 and affect RWGS equilibrium. Compared with the presence of H_2O, the existing O_2 has a more negative impact on ICCU-RWGS. The presence of O_2 would significantly decrease CO_2 conversion owing to the oxidation of catalytic sites.

The CO_2 concentration could affect not only the performance of CO_2 adsorption, but also the following RWGS process. With the increase of CO_2 concentration from 5.8% to 9.5%, the efficiency of CO_2 capture and CO_2 conversion slightly decreased at temperatures under 450 °C, *i.e.* from 100% to 98% and from 80% to 67%, respectively. In contrast, CO selectivity was increased from 90% to 92%.[71]

4.2 Development of DFM progress for ICCU-RWGS

4.2.1 Adsorbents in DFMs for ICCU-RWGS. CaO, a cheap and abundant adsorbent with excellent CO_2 capacity, has been widely used in ICCU-RWGS due to its mature application in calcium chemical looping. In order to alleviate the sintering of CaO in cyclic adsorption and desorption, constructing a porous structure or better dispersion helps to improve the cycle performance of the adsorbent. The sol–gel method is a simple and effective way to synthesize porous materials, and was applied by Shao *et al.*[72] and Sun *et al.*[73]

In addition, introducing materials with high thermal stability also helps to limit excessive sintering of CaO. Sun *et al.*[73] reported that introducing CeO_2 as a physical barrier retarded the sintering of CaO. Similarly, Shao *et al.*[72] achieved impressive cycle stability (no decrease after 10 cycles) by adding MgO into the DFMs.

Apart from the widely used CaO, hydrotalcite could also be a potential adsorbent, due to its structural stability at high temperatures. DFMs using hydrotalcite as an adsorbent showed excellent stability (stable after 750 cycles).[71]

4.2.2 Catalysts in DFMs for ICCU-RWGS. RWGS is a popular research topic due to its potential industrial application in C1 chemistry. As shown in Fig. 8, noble metals (Pt,[74–81] Ru,[82,83] Au[84,85] and Rh[86]), and Fe-based,[82,87–90] Ni-based,[91–96] Cu-based[83,97–99] and Co-based[100–102] metals are the most popular catalysts. It can be clearly observed that RWGS is favored at a higher reaction temperature. However, as shown in Fig. 8,

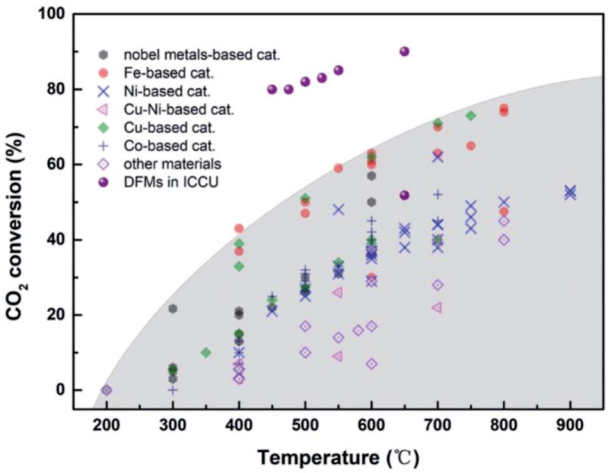

Fig. 8 CO_2 conversion of RWGS[39,74,76–88,90–92,94–117] and integrated CO_2 capture and RWGS.[71–73]

there are obvious equilibrium limitations that limit the possibility of obtaining syngas with high purity from traditional RWGS. ICCU-RWGS can be the solution to facilitate the application of RWGS. Due to the unique reaction mechanism of ICCU, RWGS can be carried out at high hydrogen concentration, making it possible to obtain a high CO_2 conversion and produce high-purity syngas.

In the existing ICCU-RWGS research work, transition metal-based catalysts have shown excellent catalytic performance. Shao *et al.*[72] applied bimetallic Fe^{3+}/Fe^{2+} and Co^{3+}/Co^{2+} redox couples in a hierarchical porous CaO/MgO composite and achieved an excellent ICCU-RWGS performance. The bimetallic couples significantly lowered the electric potential difference of Fe^{3+}/Fe^{2+} through the newly formed Fermi level in $Fe_5Co_5Mg_{10}CaO$, which made the electron spillover easier to improve the catalytic activity. It was suggested that the same content of Fe and Co could achieve optimal ICCU-RWGS performance. The authors also proposed that Fe^{2+} was the active catalytic site, whereas Co acted as the catalytic promoter in $Fe_5Co_5Mg_{10}CaO$ DFMs. The catalytic process is as follows: firstly, CO_2 was catalytically reduced to CO by magnetite (Fe_3O_4). Secondly, hematite (Fe_2O_3) was regenerated by H_2 with Co as the promoter. The well-dispersed Fe can ensure the continuous and efficient process of this catalytic process. Luis *et al.*[71] synthesized FeCrCu/K/MgO–Al_2O_3 DFMs for ICCU-RWGS under realistic conditions, and the key functions of Cu and K were suggested for efficient CO_2 reduction and capture, respectively.

Supports can also play key roles in the catalytic process by promoting and stabilizing active catalytic sites. Sun *et al.*[73] synthesized Ni–CeO_2/CaO DFMs and achieved almost 100% CO selectivity, 51.8% CO_2 conversion and remarkable cycle stability after 20 cycles of ICCU. The oxygen vacancies and interaction between Ni and CeO_2 were believed to play key roles in promoting ICCU-RWGS. It was suggested that the formed interaction would effectively retard the agglomeration of NiO.

5. Progress in low temperature ICCU

The widely applied CO_2 capture (*i.e.* MEA adsorption and calcium looping) and utilization (*i.e.* CO_2 methanation and RWGS) consume a large amount of energy for sorbent regeneration and CO_2 conversion. To overcome the drawbacks of the above processes, many researchers paid attention to photo-, electronic- and plasma-promoted catalytic processes. The integrated process can achieve promising performance under more mild conditions (ambient temperature and pressure) with the introduction of photo, electronic or plasma energy.

The traditional CO_2 capture and utilization process can achieve excellent process efficiency. However, it needs either high temperature (>500 °C) or high pressure (>20 bar). Furthermore, these processes required relatively expensive reducing agents (*i.e.* H_2 and CH_4) to convert CO_2. Alternatively, photo-catalytic reduction of CO_2 with H_2O has emerged as a promising option.[118] Hybrid MgAl(LDO)/TiO_2,[118] NH_2-UiO-66/TiO_2,[119] $Mg(OH)_2$/CuO/Cu_2O,[120] *etc.* are applied in integrated CO_2 capture and utilization and achieved promising results. Imidazolium ionic liquids, imidazolylidene heterocyclic carbenes, and zeolitic imidazolate frameworks are also commonly used materials to realize this process.[33] Integrated CO_2 capture and photo-catalytic conversion provide a sustainable solution for CO_2 emission reduction and utilization, which faces challenges in the improvement of catalytic efficiency.

The electrocatalytic CO_2 reduction reaction (CO_2RR) to produce valuable chemicals with renewable energy inputs is an attractive route to convert intermittent green energy sources.[121–123] The CO_2RR remains a huge challenge due to multiple proton and electron transfer processes and the chemical inertness of CO_2 molecules.[124] Therefore, many researchers developed various finely designed materials to improve the efficiency of CO_2 conversion. For example, Jiang *et al.*[124] applied a wet chemistry and pyrolysis method to synthesize Sb SA/NC and achieved efficient formate production (faradaic efficiency of 94.0% at −0.8 V *vs.* RHE). Recently, Lee *et al.*[125] achieved an electrochemical upgrade of CO_2 from amine capture solution, promising progress in large-scale application of integrated CO_2 capture and electrocatalytic conversion. Electrocatalysis has a very high energy utilization efficiency. The possible drawbacks are the high requirements for the purity of the reactants to avoid the poisoning effect of impurities on the catalysts and equipment.[126]

Non-thermal plasma (NTP) catalyzed CO_2 conversion has also become a promising method to significantly reduce the reaction temperature because plasma can activate CO_2 at room temperatures and atmospheric pressure.[29,32] In addition to DFMs containing adsorbents and catalysts, the membrane reactor is also gaining researchers' attention. Chen *et al.*[127] realized integrated CO_2 membrane separation and NTP CO_2 conversion with 91.8% carbon capture efficiency and 71.7% carbon utilization efficiency. This integrated process was also verified by Li *et al.*[128] ICCU with NTP can achieve excellent reaction efficiency and scalable CO_2 throughput. However, energy consumption related to NTP-ICCU needs to be particularly investigated.

Nowadays, low-temperature ICCU has gradually become a promising direction, and many finely designed materials are used in ICCU under mild conditions and have achieved excellent catalytic performance. CO_2 reduction and neutralization should deal with a concentrated CO_2 in industry (*i.e.* power plants and cement factories), which requires high CO_2 throughput. High material costs may not be suitable for large-scale processing, and the resistance to impurities in the CO_2 sources will also determine the availability of related CCU technologies.

6. Conclusions and prospects

In this paper, we have critically reviewed the state-of-the-art progress in integrated high temperature CO_2 capture and catalytic conversion, including CO_2 methanation, DRM and RWGS, from the perspective of process parameters and catalytic materials. This process can not only decrease the overall CO_2 utilization cost by eliminating CO_2 enrichment and transportation, but also achieve outstanding CO_2 conversion performance owing to the reducing agent rich conditions. However, there are several research gaps in this field that need to be addressed. For example, comprehensive considerations from the perspective of engineering are needed, including process design, and economic and technical analysis. The energy consumption for high temperature operations is noteworthy. Therefore, developing low-cost materials that can process ICCU at lower temperatures is promising. Furthermore, more research is needed for the development of dual functional catalysts for application in ICCU, including an in-depth understanding of the synergies between catalysts and adsorbents in addition to reaction intermediates.

For ICCU-methanation, an intermediate process temperature (~300 °C) shows better catalytic activity and CH_4 selectivity. Ni-based DFMs can achieve excellent ICCU-methanation performance only in the absence of O_2. The noble metal-based DFMs can obtain impressive ICCU performance, however, with inevitable high cost. The spillover of CO_2 from adsorbents to catalytic sites is a key step for ICCU-methanation, which can be promoted by the interactions between adsorbents and catalysts. More research on the interactions within DFMs is necessary for a better understanding of the ICCU-methanation process and effective catalyst design. Furthermore, an economic evaluation will guide the development of ICCU-methanation.

For ICCU-DRM, a high temperature (>500 °C) is necessary to promote reactions. Therefore, both CaO and Ni are applicable and affordable. The reaction time is a critical parameter to control the coke formation in DFMs and optimize the H_2/CO ratio of syngas in ICCU-DRM. The sintering of CaO and active metals at high temperatures is usually the main reason for the decrease of catalytic activity owing to the coverage of active sites and agglomeration of metals. The environmentally unfriendly CO generated from the coke in DFMs in the adsorption step is also worthy of attention.

ICCU-RWGS is a promising integrated process owing to its lower Gibbs energy and excellent selectivity of syngas. The

ICCU-RWGS process shows great potential for surpassing the equilibrium limitation of CO_2 conversion in traditional RWGS. The interaction among different components within DFMs plays multifunctional roles in ICCU-RWGS, including prohibiting the sintering of adsorbents, dispersing active metals and providing active sites. Apart from the investigation on the interaction within DFMs, the H_2/CO ratio of syngas from ICCU-RWGS also deserves more attention.

In conclusion, CO_2 capture and *in situ* catalytic conversion are still in their infancy. Reducing CO_2 emissions is not necessarily a high-cost industry. In contrast, it is possible to generate economic benefits through industrial integration. ICCU provides an economic CO_2 utilization strategy, which can integrate the abundant research on CO_2 capture and conversion and provide a solution for an urgent environmental need. The integration of CO_2 capture and utilization can also be expanded to other processes, including producing methanol or other valuable C_2+ chemicals. By producing more valuable chemicals, ICCU has the potential to be profitably accompanied by CO_2 emission reduction.

Conflicts of interest

There are no conflicts to declare.

Acknowledgements

The authors gratefully acknowledge financial support from the China Scholarship Council (reference number: 201906450023). This project has received funding from the European Union's Horizon 2020 research and innovation programme under the Marie Skłodowska-Curie grant agreement No 823745.

Notes and references

1 S. M. Kim, P. M. Abdala, M. Broda, D. Hosseini, C. Coperet and C. Muller, *ACS Catal.*, 2018, **8**, 2815–2823.
2 S. Tian, F. Yan, Z. Zhang and J. Jiang, *Sci. Adv.*, 2019, **5**, eaav5077.
3 Y. L. Zhao, B. Jin and Z. W. Liang, *Ind. Eng. Chem. Res.*, 2020, **59**, 1298–1307.
4 W. Gao, S. Liang, R. Wang, Q. Jiang, Y. Zhang, Q. Zheng, B. Xie, C. Y. Toe, X. Zhu and J. Wang, *Chem. Soc. Rev.*, 2020, 8584–8686.
5 S. J. Wang, G. D. Li and C. L. Fang, *Renewable Sustainable Energy Rev.*, 2018, **81**, 2144–2159.
6 R. N. E. Huaman and T. X. Jun, *Renewable Sustainable Energy Rev.*, 2014, **31**, 368–385.
7 B. L. Salvi and S. Jindal, *SN Appl. Sci.*, 2019, **1**, 20.
8 R. Falkner, H. Stephan and J. Vogler, *Glob. Policy*, 2010, **1**, 252–262.
9 R. Falkner, *Int. Aff.*, 2016, **92**, 1107–1125.
10 G. Scheffknecht, L. Al-Makhadmeh, U. Schnell and J. Maier, *Int. J. Greenhouse Gas Control*, 2011, **5**, S16–S35.
11 E. I. Koytsoumpa, C. Bergins and E. Kakaras, *J. Supercrit. Fluids*, 2018, **132**, 3–16.
12 M. E. Boot-Handford, J. C. Abanades, E. J. Anthony, M. J. Blunt, S. Brandani, N. Mac Dowell, J. R. Fernandez, M. C. Ferrari, R. Gross, J. P. Hallett, R. S. Haszeldine, P. Heptonstall, A. Lyngfelt, Z. Makuch, E. Mangano, R. T. J. Porter, M. Pourkashanian, G. T. Rochelle, N. Shah, J. G. Yao and P. S. Fennell, *Energy Environ. Sci.*, 2014, **7**, 130–189.
13 M. D. Aminu, S. A. Nabavi, C. A. Rochelle and V. Manovic, *Appl. Energy*, 2017, **208**, 1389–1419.
14 A. Sanna, M. Uibu, G. Caramanna, R. Kuusik and M. M. Maroto-Valer, *Chem. Soc. Rev.*, 2014, **43**, 8049–8080.
15 Y. Zheng, W. Q. Zhang, Y. F. Li, J. Chen, B. Yu, J. C. Wang, L. Zhang and J. J. Zhang, *Nano Energy*, 2017, **40**, 512–539.
16 M. Bui, C. S. Adjiman, A. Bardow, E. J. Anthony, A. Boston, S. Brown, P. S. Fennell, S. Fuss, A. Galindo, L. A. Hackett, J. P. Hallett, H. J. Herzog, G. Jackson, J. Kemper, S. Krevor, G. C. Maitland, M. Matuszewski, I. S. Metcalfe, C. Petit, G. Puxty, J. Reimer, D. M. Reiner, E. S. Rubin, S. A. Scott, N. Shah, B. Smit, J. P. M. Trusler, P. Webley, J. Wilcox and N. Mac Dowell, *Energy Environ. Sci.*, 2018, **11**, 1062–1176.
17 Y. A. Criado, B. Arias and J. C. Abanades, *Energy Environ. Sci.*, 2017, **10**, 1994–2004.
18 S. Fakher and A. Imqam, *Fuel*, 2020, 265.
19 M. van der Spek, S. Roussanaly and E. S. Rubin, *Int. J. Greenhouse Gas Control*, 2019, **83**, 91–104.
20 M. Zhao, A. I. Minett and A. T. Harris, *Energy Environ. Sci.*, 2013, **6**, 25–40.
21 B. A. Seibel and P. J. Walsh, *Science*, 2001, **294**, 319–320.
22 J. C. Abanades, E. S. Rubin, M. Mazzotti and H. J. Herzog, *Energy Environ. Sci.*, 2017, **10**, 2491–2499.
23 B. Yao, T. Xiao, O. A. Makgae, X. Jie, S. Gonzalez-Cortes, S. Guan, A. I. Kirkland, J. R. Dilworth, H. A. Al-Megren and S. M. Alshihri, *Nat. Commun.*, 2020, **11**, 1–12.
24 R. Sen, A. Goeppert, S. Kar and G. S. Prakash, *J. Am. Chem. Soc.*, 2020, **142**, 4544–4549.
25 P. Bareschino, E. Mancusi, M. Urciuolo, A. Paulillo, R. Chirone and F. Pepe, *Renewable Sustainable Energy Rev.*, 2020, **130**, 12.
26 M. Jouny, J.-J. Lv, T. Cheng, B. H. Ko, J.-J. Zhu, W. A. Goddard and F. Jiao, *Nat. Chem.*, 2019, **11**, 846–851.
27 H. X. Zhong, J. Wang, Q. Zhang, F. Meng, D. Bao, T. Liu, X. Y. Yang, Z. W. Chang, J. M. Yan and X. B. Zhang, *Adv. Sustainable Syst.*, 2017, **1**, 1700020.
28 D. Bao, Q. Zhang, F. L. Meng, H. X. Zhong, M. M. Shi, Y. Zhang, J. M. Yan, Q. Jiang and X. B. Zhang, *Adv. Mater.*, 2017, **29**, 1604799.
29 M. Moss, D. G. Reed, R. W. Allen and P. Styring, *Front. Energy Res.*, 2017, **5**, 20.
30 C. Chen, X. Zhu, X. Wen, Y. Zhou, L. Zhou, H. Li, L. Tao, Q. Li, S. Du and T. Liu, *Nat. Chem.*, 2020, **12**, 717–724.
31 H. C. Fu, F. You, H. R. Li and L. N. He, *Front. Chem.*, 2019, **7**, 15.
32 A. George, B. Shen, M. Craven, Y. Wang, D. Kang, C. Wu and X. Tu, *Renewable Sustainable Energy Rev.*, 2021, **135**, 109702.
33 S. Wang and X. Wang, *Angew. Chem., Int. Ed.*, 2016, **55**, 2308–2320.

34 M. A. A. Aziz, A. A. Jalil, S. Triwahyono and A. Ahmad, *Green Chem.*, 2015, **17**, 2647–2663.
35 P. Frontera, A. Macario, M. Ferraro and P. Antonucci, *Catalysts*, 2017, **7**, 28.
36 D. Pakhare and J. Spivey, *Chem. Soc. Rev.*, 2014, **43**, 7813–7837.
37 M. S. Fan, A. Z. Abdullah and S. Bhatia, *ChemCatChem*, 2009, **1**, 192–208.
38 X. Su, X. L. Yang, B. Zhao and Y. Q. Huang, *J. Energy Chem.*, 2017, **26**, 854–867.
39 Y. A. Daza and J. N. Kuhn, *RSC Adv.*, 2016, **6**, 49675–49691.
40 R. G. Grim, Z. Huang, M. T. Guarnieri, J. R. Ferrell, L. Tao and J. A. Schaidle, *Energy Environ. Sci.*, 2020, **13**, 472–494.
41 A. Bermejo-Lopez, B. Pereda-Ayo, J. A. Gonzalez-Marcos and J. R. Gonzalez-Velasco, *J. CO_2 Util.*, 2019, **34**, 576–587.
42 Z. J. Zhou, N. N. Sun, B. D. Wang, Z. H. Han, S. C. Cao, D. Hu, T. Y. Zhu, Q. Shen and W. Wei, *ChemSusChem*, 2020, **13**, 360–368.
43 S. B. Jo, J. H. Woo, J. H. Lee, T. Y. Kim, H. I. Kang, S. C. Lee and J. C. Kim, *Sustainable Energy Fuels*, 2020, **4**, 4679–4687.
44 Q. H. Zheng, R. Farrauto and A. C. Nguyen, *Ind. Eng. Chem. Res.*, 2016, **55**, 6768–6776.
45 M. S. Duyar, M. A. A. Treviño and R. J. Farrauto, *Appl. Catal., B*, 2015, **168–169**, 370–376.
46 M. S. Duyar, S. X. Wang, M. A. Arellano-Trevino and R. J. Farrauto, *J. CO_2 Util.*, 2016, **15**, 65–71.
47 C. V. Miguel, M. A. Soria, A. Mendes and L. M. Madeira, *Chem. Eng. J.*, 2017, **322**, 590–602.
48 S. X. Wang, E. T. Schrunk, H. Mahajan and R. J. Farrauto, *Catalysts*, 2017, **7**, 88.
49 S. X. Wang, R. J. Farrauto, S. Karp, J. H. Jeon and E. T. Schrunk, *J. CO_2 Util.*, 2018, **27**, 390–397.
50 M. A. Arellano-Trevino, Z. Y. He, M. C. Libby and R. J. Farrauto, *J. CO_2 Util.*, 2019, **31**, 143–151.
51 M. A. Arellano-Trevino, N. Kanani, C. W. Jeong-Potter and R. J. Farrauto, *Chem. Eng. J.*, 2019, **375**, 8.
52 A. Bermejo-Lopez, B. Pereda-Ayo, J. A. Gonzalez-Marcos and J. R. Gonzalez-Velasco, *Appl. Catal., B*, 2019, **256**, 11.
53 H. Sun, Y. Wang, S. Xu, A. I. Osman, G. Stenning, J. Han, S. Sun, D. Rooney, P. T. Williams and F. Wang, *Fuel*, 2020, **286**, 119308.
54 H. Sun, Y. Zhang, S. Guan, J. Huang and C. Wu, *J. CO_2 Util.*, 2020, **38**, 262–272.
55 G. Li, P. Xiao, P. A. Webley, J. Zhang and R. Singh, *Energy Procedia*, 2009, **1**, 1123–1130.
56 J. Gao, Y. Wang, Y. Ping, D. Hu, G. Xu, F. Gu and F. Su, *RSC Adv.*, 2012, **2**, 2358–2368.
57 C. J. Keturakis, F. Ni, M. Spicer, M. G. Beaver, H. S. Caram and I. E. Wachs, *ChemSusChem*, 2014, **7**, 3459–3466.
58 Q. Pan, J. Peng, T. Sun, S. Wang and S. Wang, *Catal. Commun.*, 2014, **45**, 74–78.
59 L. Proano, E. Tello, M. A. Arellano-Trevino, S. X. Wang, R. J. Farrauto and M. Cobo, *Appl. Surf. Sci.*, 2019, **479**, 25–30.
60 W. Wang and J. L. Gong, *Front. Chem. Sci. Eng.*, 2011, **5**, 2–10.
61 A. E. Aksoylu, A. N. Akin, Z. İ. Önsan and D. L. Trimm, *Appl. Catal., A*, 1996, **145**, 185–193.
62 S. Cimino, F. Boccia and L. Lisi, *J. CO_2 Util.*, 2020, **37**, 195–203.
63 S. Bhavsar and G. Veser, *RSC Adv.*, 2014, **4**, 47254–47267.
64 E. Ramirez-Cabrera, A. Atkinson and D. Chadwick, *Appl. Catal., B*, 2004, **47**, 127–131.
65 M. Usman, W. Daud and H. F. Abbas, *Renewable Sustainable Energy Rev.*, 2015, **45**, 710–744.
66 S. Molina-Ramírez, M. Cortés-Reyes, C. Herrera, M. A. Larrubia and L. J. Alemany, *J. CO_2 Util.*, 2020, 40.
67 A. Al-Mamoori, A. A. Rownaghi and F. Rezaei, *ACS Sustainable Chem. Eng.*, 2018, **6**, 13551–13561.
68 J. M. Lavoie, *Front. Chem.*, 2014, **2**, 81.
69 M. D. Porosoff, B. Yan and J. G. Chen, *Energy Environ. Sci.*, 2016, **9**, 62–73.
70 A. Y. Khodakov, W. Chu and P. Fongarland, *Chem. Rev.*, 2007, **107**, 1692–1744.
71 L. F. Bobadilla, J. M. Riesco-Garcia, G. Penelas-Perez and A. Urakawa, *J. CO_2 Util.*, 2016, **14**, 106–111.
72 B. Shao, G. Hu, K. A. Alkebsi, G. Ye, X. Lin, W. Du, J. Hu, M. Wang, H. Liu and F. Qian, *Energy Environ. Sci.*, 2021, 2291–2301.
73 H. Sun, J. Wang, J. Zhao, B. Shen, J. Shi, J. Huang and C. Wu, *Appl. Catal., B*, 2019, **244**, 63–75.
74 A. Goguet, F. Meunier, J. P. Breen, R. Burch, M. I. Petch and A. F. Ghenciu, *J. Catal.*, 2004, **226**, 382–392.
75 G. Jacobs and B. H. Davis, *Appl. Catal., A*, 2005, **284**, 31–38.
76 G. S. Yablonsky, R. Pilasombat, J. P. Breen, R. Burch and S. Hengrasmee, *Chem. Eng. Sci.*, 2010, **65**, 2325–2332.
77 S. S. Kim, H. H. Lee and S. C. Hong, *Appl. Catal., B*, 2012, **119**, 100–108.
78 S. S. Kim, K. H. Park and S. C. Hong, *Fuel Process. Technol.*, 2013, **108**, 47–54.
79 X. D. Chen, X. Su, H. M. Duan, B. L. Liang, Y. Q. Huang and T. Zhang, *Catal. Today*, 2017, **281**, 312–318.
80 X. L. Yang, X. Su, X. D. Chen, H. M. Duan, B. L. Liang, Q. G. Liu, X. Y. Liu, Y. J. Ren, Y. Q. Huang and T. Zhang, *Appl. Catal., B*, 2017, **216**, 95–105.
81 S. M. Lee, H. Eom and S. S. Kim, *Environ. Technol.*, 2019, **42**, 182–192.
82 C. Panaritis, M. Edake, M. Couillard, R. Einakchi and E. A. Baranova, *J. CO_2 Util.*, 2018, **26**, 350–358.
83 Y. C. Zhuang, R. Currie, K. B. McAuley and D. S. A. Simakov, *Appl. Catal., A*, 2019, **575**, 74–86.
84 W. Benzinger, E. Daymo, M. Hettel, L. Maier, C. Antinori, P. Pfeifer and O. Deutschmann, *Chem. Eng. J.*, 2019, **362**, 430–441.
85 N. Ishito, K. Hara, K. Nakajima and A. Fukuoka, *J. Energy Chem.*, 2016, **25**, 306–310.
86 J. C. Matsubu, V. N. Yang and P. Christopher, *J. Am. Chem. Soc.*, 2015, **137**, 3076–3084.
87 A. G. Kharaji, A. Shariati and M. A. Takassi, *Chin. J. Chem. Eng.*, 2013, **21**, 1007–1014.
88 D. H. Kim, S. W. Han, H. S. Yoon and Y. D. Kim, *J. Ind. Eng. Chem.*, 2015, **23**, 67–71.
89 J. A. Loiland, M. J. Wulfers, N. S. Marinkovic and R. F. Lobo, *Catal. Sci. Technol.*, 2016, **6**, 5267–5279.

90 L. Pastor-Perez, M. Shah, E. le Sache and T. R. Reina, *Catalysts*, 2018, **8**, 608.
91 B. Lu and K. Kawamoto, *J. Environ. Chem. Eng.*, 2013, **1**, 300–309.
92 L. H. Wang, H. Liu, Y. Liu, Y. Chen and S. Q. Yang, *J. Rare Earths*, 2013, **31**, 969–974.
93 L. H. Wang, H. Liu, Y. Liu, Y. Chen and S. Q. Yang, *J. Rare Earths*, 2013, **31**, 559–564.
94 P. C. Zonetti, S. Letichevsky, A. B. Gaspar, E. F. Sousa-Aguiar and L. G. Appel, *Appl. Catal., A*, 2014, **475**, 48–54.
95 M. Lortie, R. Isaifan, Y. Liu and S. Mommers, *Int. J. Chem. Eng.*, 2015, **2015**, 750689.
96 M. Lortie and R. J. Isaifan, *J. Catal.*, 2015, **2015**, 1–9.
97 C. A. Galvan, J. Schumann, M. Behrens, J. L. G. Fierro, R. Schlogl and E. Frei, *Appl. Catal., B*, 2016, **195**, 104–111.
98 X. Zhang, X. B. Zhu, L. L. Lin, S. Y. Yao, M. T. Zhang, X. Liu, X. P. Wang, Y. W. Li, C. Shi and D. Ma, *ACS Catal.*, 2017, **7**, 912–918.
99 G. L. Zhou, B. C. Dai, H. M. Xie, G. Z. Zhang, K. Xiong and X. X. Zheng, *J. CO_2 Util.*, 2017, **21**, 292–301.
100 L. H. Wang, H. Liu, Y. Chen and S. Q. Yang, *Int. J. Hydrogen Energy*, 2017, **42**, 3682–3689.
101 Y. L. Shen, Z. Cao and Z. H. Xiao, *Catalysts*, 2019, **9**, 423.
102 L. H. Wang and H. Liu, *Catal. Today*, 2018, **316**, 155–161.
103 B. L. Liang, H. M. Duan, X. Su, X. D. Chen, Y. Q. Huang, X. W. Chen, J. J. Delgado and T. Zhang, *Catal. Today*, 2017, **281**, 319–326.
104 Z. S. Fishman, Y. L. He, K. R. Yang, A. W. Lounsbury, J. Q. Zhu, T. M. Tran, J. B. Zimmerman, V. S. Batista and L. D. Pfefferle, *Nanoscale*, 2017, **9**, 12984–12995.
105 J. A. Loiland, M. J. Wulfers, N. S. Marinkovic and R. F. Lobo, *Catal. Sci. Technol.*, 2016, **6**, 5267–5279.
106 L. Pastor-Perez, F. Baibars, E. Le Sache, H. Arellano-Garcia, S. Gu and T. R. Reina, *J. CO_2 Util.*, 2017, **21**, 423–428.
107 A. Ranjbar, A. Irankhah and S. F. Aghamiri, *J. Environ. Chem. Eng.*, 2018, **6**, 4945–4952.
108 A. M. Bahmanpour, F. Heroguel, M. Kilic, C. J. Baranowski, L. Artiglia, U. Rothlisberger, J. S. Luterbacher and O. Krocher, *ACS Catal.*, 2019, **9**, 6243–6251.
109 F. M. Sun, C. F. Yan, Z. D. Wang, C. Q. Guo and S. L. Huang, *Int. J. Hydrogen Energy*, 2015, **40**, 15985–15993.
110 N. Nityashree, C. A. H. Price, L. Pastor-Perez, G. V. Manohara, S. Garcia, M. M. Maroto-Valer and T. R. Reina, *Appl. Catal., B*, 2020, 261.
111 L. Wang, H. Liu, Y. Chen, R. Zhang and S. Yang, *Chem. Lett.*, 2013, **42**, 682–683.
112 Q. D. Sun, J. Y. Ye, C. J. Liu and Q. F. Ge, *Greenhouse Gases: Sci. Technol.*, 2014, **4**, 140–144.
113 Y. L. He, K. R. Yang, Z. W. Yu, Z. S. Fishman, L. A. Achola, Z. M. Tobin, J. A. Heinlein, S. Hu, S. L. Suib, V. S. Batista and L. D. Pfefferle, *Nanoscale*, 2019, **11**, 16677–16688.
114 W. Wang, Y. Zhang, Z. Y. Wang, J. M. Yan, Q. F. Ge and C. J. Liu, *Catal. Today*, 2016, **259**, 402–408.
115 Q. Zhang, L. Pastor-Perez, W. Jin, S. Gu and T. R. Reina, *Appl. Catal., B*, 2019, **244**, 889–898.
116 F. G. Baddour, E. J. Roberts, A. T. To, L. Wang, S. E. Habas, D. A. Ruddy, N. M. Bedford, J. Wright, C. P. Nash, J. A. Schaidle, R. L. Brutchey and N. Malmstadt, *J. Am. Chem. Soc.*, 2020, **142**, 1010–1019.
117 J. R. Morse, M. Juneau, J. W. Baldwin, M. D. Porosoff and H. D. Willauer, *J. CO_2 Util.*, 2020, **35**, 38–46.
118 L. Liu, C. Zhao, J. Xu and Y. Li, *Appl. Catal., B*, 2015, **179**, 489–499.
119 A. Crake, K. C. Christoforidis, A. Kafizas, S. Zafeiratos and C. Petit, *Appl. Catal., B*, 2017, **210**, 131–140.
120 M. Flores-Flores, E. Luévano-Hipólito, L. M. Torres-Martínez and T.-O. Do, *Mater. Chem. Phys.*, 2019, **227**, 90–97.
121 X. Zhao, L. Du, B. You and Y. Sun, *Catal. Sci. Technol.*, 2020, **10**, 2711–2720.
122 K. Liu, J. Wang, M. Shi, J. Yan and Q. Jiang, *Adv. Energy Mater.*, 2019, **9**, 1900276.
123 K.-H. Liu, H.-X. Zhong, X.-Y. Yang, D. Bao, F.-L. Meng, J.-M. Yan and X.-B. Zhang, *Green Chem.*, 2017, **19**, 4284–4288.
124 Z. Jiang, T. Wang, J. Pei, H. Shang, D. Zhou, H. Li, J. Dong, Y. Wang, R. Cao and Z. Zhuang, *Energy Environ. Sci.*, 2020, **13**, 2856–2863.
125 G. Lee, Y. C. Li, J.-Y. Kim, T. Peng, D.-H. Nam, A. S. Rasouli, F. Li, M. Luo, A. H. Ip and Y.-C. Joo, *Nat. Energy*, 2021, **6**, 46–53.
126 S. M. Tan and M. Pumera, *ACS Nano*, 2019, **13**, 2681–2728.
127 H. Chen, Y. Mu, C. Hardacre and X. Fan, *Ind. Eng. Chem. Res.*, 2020, **59**, 8202–8211.
128 S. Li, M. Ongis, G. Manzolini and F. Gallucci, *Chem. Eng. J.*, 2021, **410**, 128335.